



**HAL**  
open science

## Recent trends in the chemistry of major northern rivers signal widespread Arctic change

Suzanne Tank, James Mcclelland, Robert Spencer, Alexander Shiklomanov,  
Anya Suslova, Florentina Moatar, Rainer Amon, Lee Cooper, Greg Elias,  
Vyacheslav Gordeev, et al.

### ► To cite this version:

Suzanne Tank, James Mcclelland, Robert Spencer, Alexander Shiklomanov, Anya Suslova, et al..  
Recent trends in the chemistry of major northern rivers signal widespread Arctic change. *Nature  
Geoscience*, 2023, 16, pp.789-796. 10.1038/s41561-023-01247-7 . hal-04198078

**HAL Id: hal-04198078**

**<https://hal.inrae.fr/hal-04198078>**

Submitted on 1 Feb 2024

**HAL** is a multi-disciplinary open access archive for the deposit and dissemination of scientific research documents, whether they are published or not. The documents may come from teaching and research institutions in France or abroad, or from public or private research centers.

L'archive ouverte pluridisciplinaire **HAL**, est destinée au dépôt et à la diffusion de documents scientifiques de niveau recherche, publiés ou non, émanant des établissements d'enseignement et de recherche français ou étrangers, des laboratoires publics ou privés.

# Long-term Trends in Arctic Riverine Chemistry Signal Multi-faceted Northern Change

**Suzanne Tank** (✉ [suzanne.tank@ualberta.ca](mailto:suzanne.tank@ualberta.ca))

University of Alberta <https://orcid.org/0000-0002-5371-6577>

**James McClelland**

Marine Biological Laboratory

**Robert Spencer**

Florida State University

**Alexander Shiklomanov**

University of New Hampshire

**Anya Suslova**

Woodwell Climate Research Center

**Florentina Moatar**

INRAE

**Rainer Amon**

Texas A&M University, Galveston Campus <https://orcid.org/0000-0002-1437-4316>

**Lee Cooper**

University of Maryland

**Greg Elias**

Western Arctic Research Center

**Vyacheslav Gordeev**

Russian Academy of Sciences

**Christopher Guay**

Mamala Research LLC

**Tatiana Gurtovaya**

South Russia Centre for Preparation and Implementation of International Projects

**Lyudmila Kosmenko**

Ministry of Natural Resources and Environment of the Russian Federation

**Edda Mutter**

Yukon River Inter-Tribal Watershed Council

**Bruce Peterson**

Marine Biological Laboratory

**Bernhard Peucker-Ehrenbrink**

Woods Hole Oceanographic Institution <https://orcid.org/0000-0002-3819-992X>

**Peter Raymond**

Yale University <https://orcid.org/0000-0002-8564-7860>

**Paul Schuster**

U.S. Geological Survey <https://orcid.org/0000-0002-8314-1372>

**Lindsay Scott**

Woodwell Climate Research Center

**Robin Staples**

Government of the Northwest Territories

**Robert Striegl**

US Geological Survey <https://orcid.org/0000-0002-8251-4659>

**Mikhail Tretiakov**

Arctic and Antarctic Research Institute <https://orcid.org/0000-0003-3702-6362>

**Alexander Zhulidov**

South Russia Centre for Preparation and Implementation of International Projects

**Nikita Zimov**

Northeast Science Station

**Sergey Zimov**

Northeast Science Station of Pacific Geographical Institute <https://orcid.org/0000-0002-0053-6599>

**Robert Holmes**

Woodwell Climate Research Center

---

**Article**

**Keywords:**

**Posted Date:** February 9th, 2023

**DOI:** <https://doi.org/10.21203/rs.3.rs-2530682/v1>

**License:**  This work is licensed under a Creative Commons Attribution 4.0 International License.

[Read Full License](#)

**Additional Declarations:** There is **NO** Competing Interest.

---

**Version of Record:** A version of this preprint was published at Nature Geoscience on August 21st, 2023. See the published version at <https://doi.org/10.1038/s41561-023-01247-7>.



41 **Abstract**

42 **Large rivers integrate processes occurring throughout their watersheds, and are therefore sentinels of**  
43 **change across broad spatial scales. Riverine chemistry also regulates ecosystem function across**  
44 **Earth’s land-ocean continuum, exerting control from the micro- (e.g., food web) to the macro- (e.g.,**  
45 **carbon cycle) scale. In the rapidly warming Arctic, a wide range of processes have been hypothesized**  
46 **to alter river water chemistry. However, it is unknown how the land-ocean flux of waterborne**  
47 **constituents is changing at the pan-Arctic scale. Here, we show profound shifts in the concentration**  
48 **and transport of biogeochemical constituents in the six largest Arctic rivers (the Ob’, Yenisey, Lena,**  
49 **Kolyma, Yukon, and Mackenzie) since 2003, near river mouths capturing two-thirds of the pan-Arctic**  
50 **watershed. While some constituent fluxes increase substantially at the pan-Arctic scale (alkalinity and**  
51 **associated ions), others decline (nitrate and associated inorganic nutrients) or are overall unchanged**  
52 **(dissolved organics). These clear but divergent trends diagnose a multi-systems perturbation that**  
53 **indicates alteration of processes ranging from chemical weathering on land, to primary production in**  
54 **the coastal ocean. We anticipate these findings will refine models of current and future functioning of**  
55 **the coupled land-ocean Arctic system, and spur research on scale-dependent change across the river-**  
56 **integrated Arctic domain.**

57

58 **Main**

59 Large rivers are planetary linchpins, connecting vast swaths of terrestrial landmass to the  
60 world’s coastal oceans. On land, rivers integrate patchy landscapes and the variable biogeochemical  
61 processes that these landscapes host, as water moving through watersheds incorporates the chemical  
62 signature of its flow path. In the coastal ocean, the chemical signature of water transported by rivers  
63 regulates nearshore biogeochemical<sup>1,2</sup> and ecological<sup>3,4</sup> function; over broader scales, river water and its  
64 composition modify ocean physics<sup>1</sup>. Nowhere is this more consequential than in the Arctic, where ~11%  
65 of Earth’s riverine discharge drains into an enclosed basin containing ~1% of global ocean volume<sup>5</sup>. This  
66 drainage occurs predominantly via six large rivers (Figure 1, Extended Data Table 1). As a result,  
67 quantifying trends in river water chemistry at a constrained series of downstream sites allows us to  
68 diagnose change across much of the pan-Arctic watershed, better understand the current functioning of  
69 the connected land-ocean Arctic system, and predict what the future may hold for this rapidly changing  
70 region<sup>6</sup>.

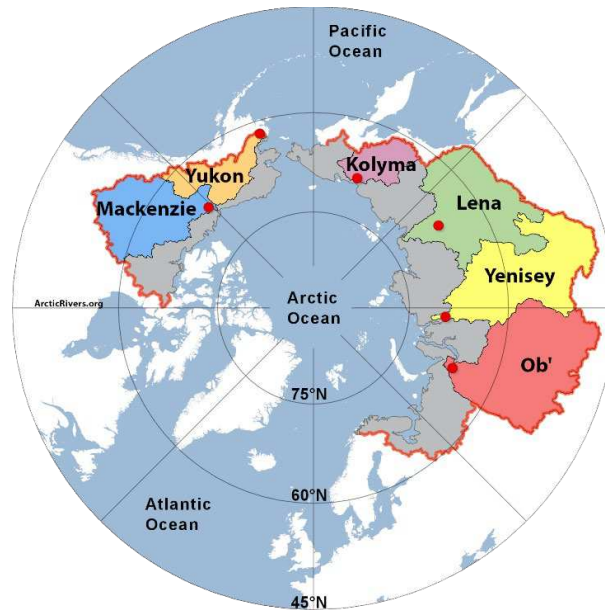


**Figure 1:** The six great Arctic rivers that are the focus of this assessment. Sampling locations are indicated by red dots. The  $16.8 \times 10^6 \text{ km}^2$  pan-Arctic watershed is delineated by the red line.

71 Past work on north-flowing rivers has established significant increases in discharge across the  
 72 pan-Arctic since the early-mid 20<sup>th</sup> century<sup>7,8</sup> (Figure 2), attributed to intensification of the hydrologic  
 73 cycle<sup>9</sup>. Such increases in water transport suggest that we should expect long-term change in the riverine  
 74 flux (i.e., total riverine transport, as mass time<sup>-1</sup>) of biogeochemical constituents, particularly for  
 75 constituents such as organic carbon that are transport, rather than supply, limited in the north<sup>10,11</sup>.  
 76 Similarly, there is a broadly articulated expectation that permafrost thaw will increase the transport of  
 77 organic matter, nutrients, and ions to aquatic networks, and thus their delivery to the coastal ocean<sup>12-14</sup>.  
 78 However, these assessments miss that change in the north is multi-faceted, with factors such as  
 79 shrubification<sup>15</sup>, temperature-induced increases in biogeochemical processing rates by heterotrophic  
 80 and autotrophic microbes<sup>16-18</sup>, disturbances such as wildfire<sup>19</sup>, and human modifications such as river  
 81 impoundment<sup>20-22</sup>, changing land use<sup>23</sup>, and changing industrial emissions<sup>24</sup> often occurring  
 82 simultaneously, with the potential for antagonistic effects<sup>e.g., 25</sup>. Even for permafrost thaw, deepening  
 83 flowpaths<sup>26</sup> or processes such as sorption<sup>27,28</sup> can lead to patterns in mobilization that vary between  
 84 sites or regions<sup>29</sup>.

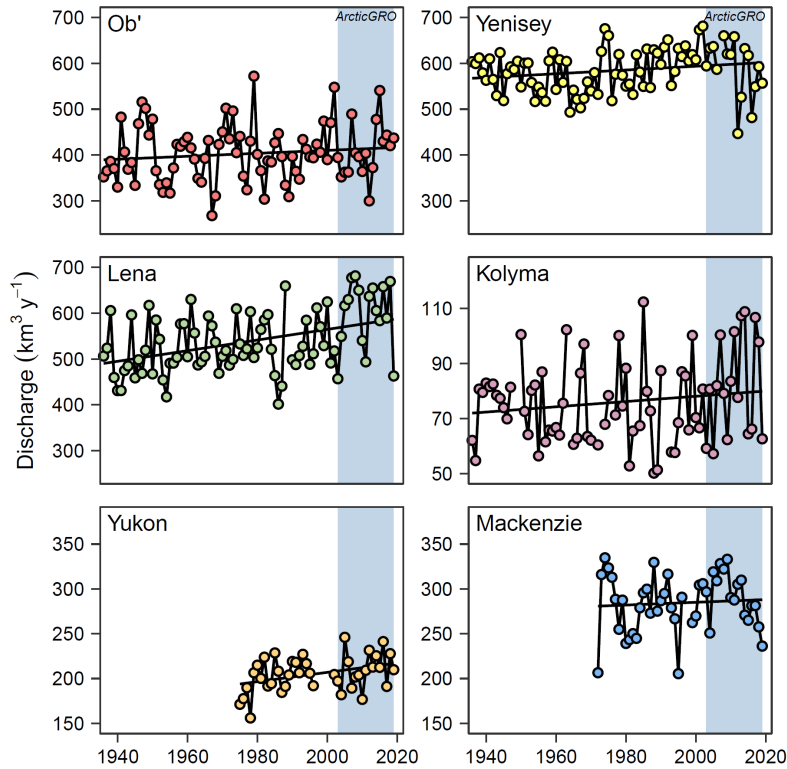


**Figure 2:** Long-term discharge record for each of the six great Arctic rivers. The timespan of the ArcticGRO data record is indicated with blue shading.

85            Here, we examine a nearly twenty-year record of coupled river discharge and chemistry  
 86 (Extended Data Figure 1) collected from the six largest rivers that drain to the Arctic Ocean. These rivers:  
 87 the Ob', Yenisey, Lena, and Kolyma in Russia, and the Mackenzie and Yukon in North America, capture  
 88 two-thirds of the Arctic Ocean watershed area (Figure 1, Extended Data Table 1). This data record is the  
 89 result of our group's ongoing efforts via the Arctic Great Rivers Observatory (ArcticGRO;  
 90 [www.arcticgreatrivers.org](http://www.arcticgreatrivers.org)), which — given the challenge of collecting methodologically-consistent and  
 91 seasonally-representative samples across these diverse jurisdictions and sites — represents an  
 92 unparalleled resource for exploring Arctic riverine change. Our analyses reveal trends at magnitudes  
 93 that signal broad-scale perturbation throughout the pan-Arctic, but with divergent trajectories that shed  
 94 light on variable mechanisms of change. We use these insights to consider potential drivers of effect and

95 the consequences of observed change, and to explore where knowledge gaps are hampering our ability  
96 to understand current and future functioning of the land-ocean Arctic system.

97

### 98 **Pronounced, but divergent trends in Arctic riverine flux**

99 We focus our assessment on three chemical constituents that are important drivers of  
100 biogeochemical function across the land-ocean Arctic domain, and that are also representative of  
101 broader constituent classes. These are: dissolved organic carbon (DOC; representative of the broader  
102 organic matter pool including organic-associated nutrients); alkalinity (representative of many dissolved  
103 ions); and nitrate ( $\text{NO}_3^-$ ; representative of dissolved inorganic nutrients, including ammonium ( $\text{NH}_4^+$ ) and  
104 silica ( $\text{SiO}_2$ )) (Extended Data Figure 2). To assess constituent flux, we applied a modelling approach that  
105 couples daily discharge data with more sporadic concentration measurements, and makes use of the  
106 known relationship between concentration and discharge to determine flux (*see Methods*)<sup>30</sup>. Of our  
107 focal suite, only alkalinity experienced a pan-Arctic (i.e., six rivers combined) increase in annual flux over  
108 our period of record (Figure 3a). Nitrate declined significantly, while DOC, which has often been a focus  
109 of study given its role as a rapid-cycling component of the contemporary carbon cycle, showed no  
110 discernable change at the pan-Arctic scale (Figure 3b-c). Change that did occur, however, was  
111 substantial, with a 32% decline in  $\text{NO}_3^-$  and an 18% increase in alkalinity over a period of 17 years. An  
112 assessment of trends in flux across the broad suite of constituents measured by the ArcticGRO program  
113 (Extended Data Figure 3) reveals patterns within constituent classes (i.e., Extended Data Figure 2) that  
114 generally track those for the focal constituents. For example, trends in flux for ions closely affiliated with  
115 alkalinity ( $\text{Ca}^{2+}$ ,  $\text{Mg}^{2+}$ ,  $\text{Li}^+$ ,  $\text{Sr}^{2+}$ ) largely tracked that constituent; nutrients ( $\text{SiO}_2$  and  $\text{NH}_4^+$ ) showed a pan-  
116 Arctic decline similar to that for  $\text{NO}_3^-$ ; and patterns for total dissolved phosphorus were similar to those  
117 for DOC. Given that these constituents are regulated by processes ranging from chemical weathering<sup>2</sup> to  
118 biological uptake<sup>16-18</sup> on land; and modify processes ranging from ocean acidification<sup>31</sup> to primary



119 production<sup>4</sup> in the coastal ocean, the ecological and biogeochemical ramifications of the changes we  
120 observe are likely profound.

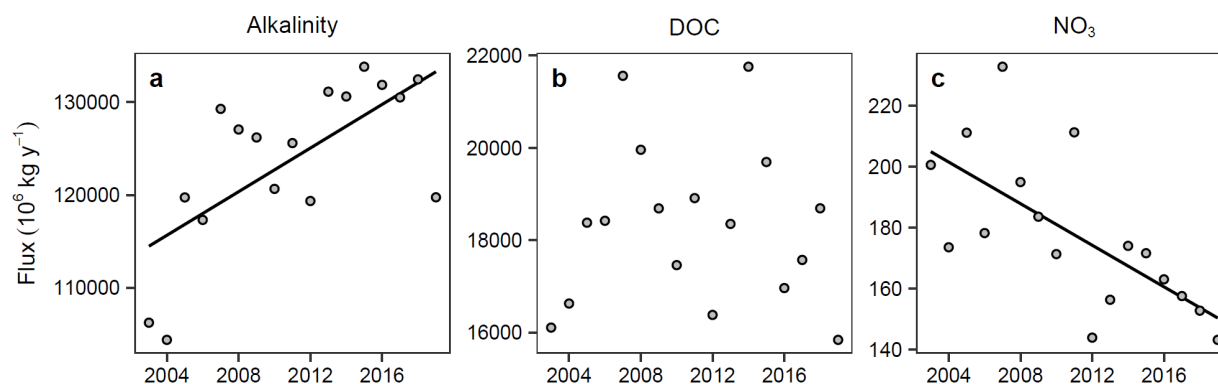


**Figure 3:** Trends in annual constituent fluxes of alkalinity (as CaCO<sub>3</sub>), dissolved organic carbon (DOC), and nitrate (as NO<sub>3</sub>-N), summed across the six great Arctic rivers. Fluxes are provided as 10<sup>6</sup> kg y<sup>-1</sup>. Thiel-Sen slopes with p<0.05 are indicated as lines within each panel. Statistical outputs are provided in Table S1.

121

122 **Concentration and discharge direct changing flux**

123 In some cases, river-specific trends in constituent flux deviated from the pan-Arctic sum. For example,

124 NO<sub>3</sub><sup>-</sup> increased modestly in the Yukon (p=0.12), and showed little change in the Ob' (p=0.70) despite the

125 pan-Arctic decline described above; alkalinity patterns for the Mackenzie (negative trend slope; p=0.54)

126 contrasted with clear increases elsewhere; and DOC increased in the Ob' and decreased in the Yenisey

127 (p<0.02) in the face of limited change in other rivers (p=0.23–0.84); (Figure 4a). In part, these patterns

128 appeared to be driven by river-specific trends in discharge, which decreased in the Mackenzie (p=0.02)

129 and Yenisey (p=0.09) over the 17-year length of our data record (Figure 4b) despite the longer-term

130 increase in discharge documented for the pan-Arctic domain<sup>7,8</sup> (Figure 2). Examining the mechanisms

131 underlying these changes in constituent flux requires that we disentangle inter-annual and long-term

132 change in water discharge from co-occurring trends in concentration. This task is complicated by the fact

133 that constituent concentrations vary seasonally and with discharge itself. We use two distinct

134 approaches to resolve these two known concerns.

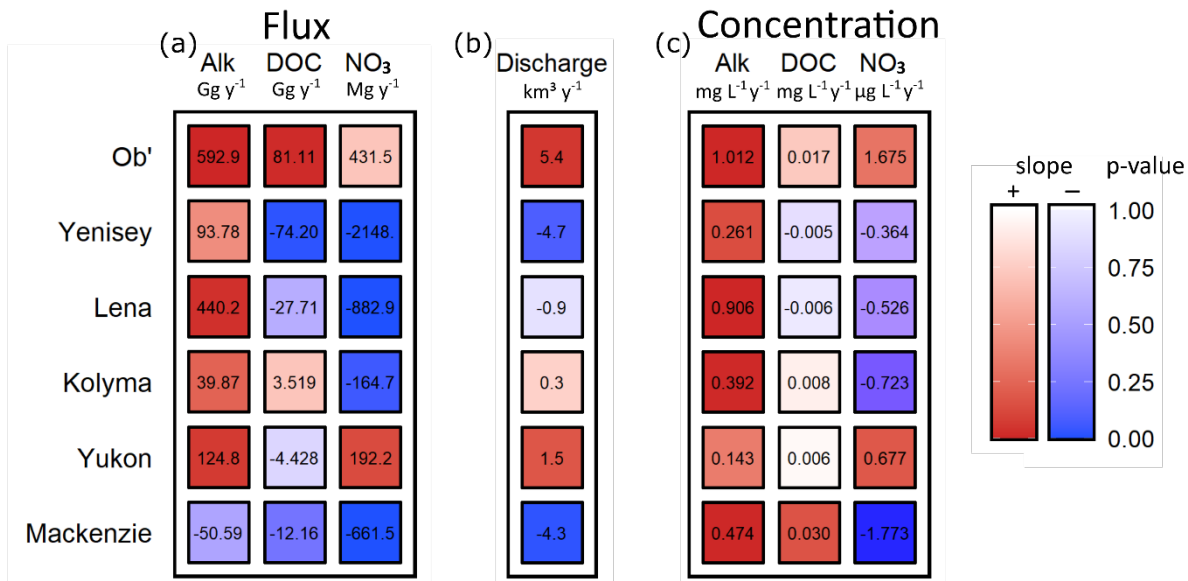


**Figure 4:** Annual trends for: (a) constituent flux; (b) discharge; and (c) concentration for each of the six great Arctic rivers. In each panel, the Sen's slope (numerical value) and p-value of the trend (shading) are shown. Flux and concentration trends for the full ArcticGRO constituent list are shown in Extended Data Figures 3 and 5, respectively; detailed statistical outputs are provided in Tables S1 and S2.

135 First, we use an approach to directly examine trends in measured concentrations, via trend  
 136 analyses that are binned by season to account for seasonal variation in concentration unrelated to  
 137 directional change over time (see *Methods*). We target this approach specifically to account for changes  
 138 to the within-year seasonality of sampling across the two-decade timespan of the ArcticGRO program.  
 139 Results from this direct trend analysis for concentration (Figure 4c) are generally similar to those for flux,  
 140 described above (Figure 4a). Increases in alkalinity are widespread ( $p=0.00$ – $0.14$  in all rivers except the  
 141 Yukon), nitrate concentrations decline (albeit modestly) across most rivers, and trends for DOC  
 142 concentration are largely absent ( $p=0.73$ – $0.96$ ) in all rivers except for the Mackenzie, where DOC  
 143 concentration increases modestly over time ( $p=0.16$ ).

144 Second, we assess changes in flux controlled for inter-annual variation in discharge via a flow-  
 145 normalization modelling approach that removes variation in discharge across years, but retains within-  
 146 year (i.e., day-to-day) seasonality. Although this method does not generate an estimate of “true” flux, it  
 147 is preferred when the analytical emphasis is mechanistic in nature (see also *Methods*)<sup>32</sup>, because it

148 overcomes year-to-year fluctuations in discharge that can obscure underlying change. These flow-  
149 normalized fluxes show trends that largely reflect those for concentration presented above (Figure 4c),  
150 with some notable refinements: increases in alkalinity and decreases in  $\text{NO}_3^-$  become more robust, and a  
151 decrease in DOC emerges for the Kolyma while the DOC increase in the Mackenzie is maintained  
152 (Extended Data Figure 4). Overall, patterns for flow-normalized fluxes are remarkably similar to our best  
153 estimates of true flux and concentration presented above, with broad-scale increases in alkalinity and  
154 declines in  $\text{NO}_3^-$ , and variable and modest trends for DOC. Taken as a whole, these broad but divergent  
155 trends diagnose a multi-systems perturbation to the pan-Arctic system, with effects profound enough to  
156 reach the mouths of large northern rivers.

157

#### 158 **Divergent trends diagnose multi-systems change**

159 The array of factors that might reasonably enable long-term change in riverine chemistry is diverse,  
160 varying regionally in magnitude and across chemical constituents in effect (Figure 5, Supplemental Text).  
161 As just one example, abrupt permafrost thaw (i.e., thermokarst) is a regionally-specific phenomena  
162 dependent on the presence of ground ice<sup>33</sup> that is generally understood to increase the transport of  
163 some constituents to riverine networks (e.g., inorganic nutrients)<sup>29</sup>, but potentially decrease others (e.g.,  
164 DOC, in cases where landscape collapse increases mineral sorption, or diverts hydrologic flow paths  
165 through mineral soils)<sup>34,35</sup>. As a result, the variation in response that we describe above can be used to  
166 diagnose drivers of change, and develop approaches to assess future functioning of the land-ocean  
167 Arctic system.

168 For some chemical constituents, known factors of change are both relatively widespread and  
169 consistent in their directionality (Figure 5; Supplemental Text). In the case of alkalinity and related ions,  
170 for example, exposure to deeper soils via either active layer deepening or thermokarst-associated  
171 permafrost thaw will typically increase mineral weathering by increasing water contact with deeper

172 mineral soils<sup>36,37</sup>. Acting synergistically, shrubification<sup>38</sup> and increased temperature-driven organic  
 173 matter processing<sup>39</sup> will increase weathering rates via processes such as increasing soil pore water  
 174 acidity. Because these processes are coherent in their directionality and geographically widespread, the  
 175 net result appears as a cohesive increase in concentration and flux throughout the pan-Arctic domain.

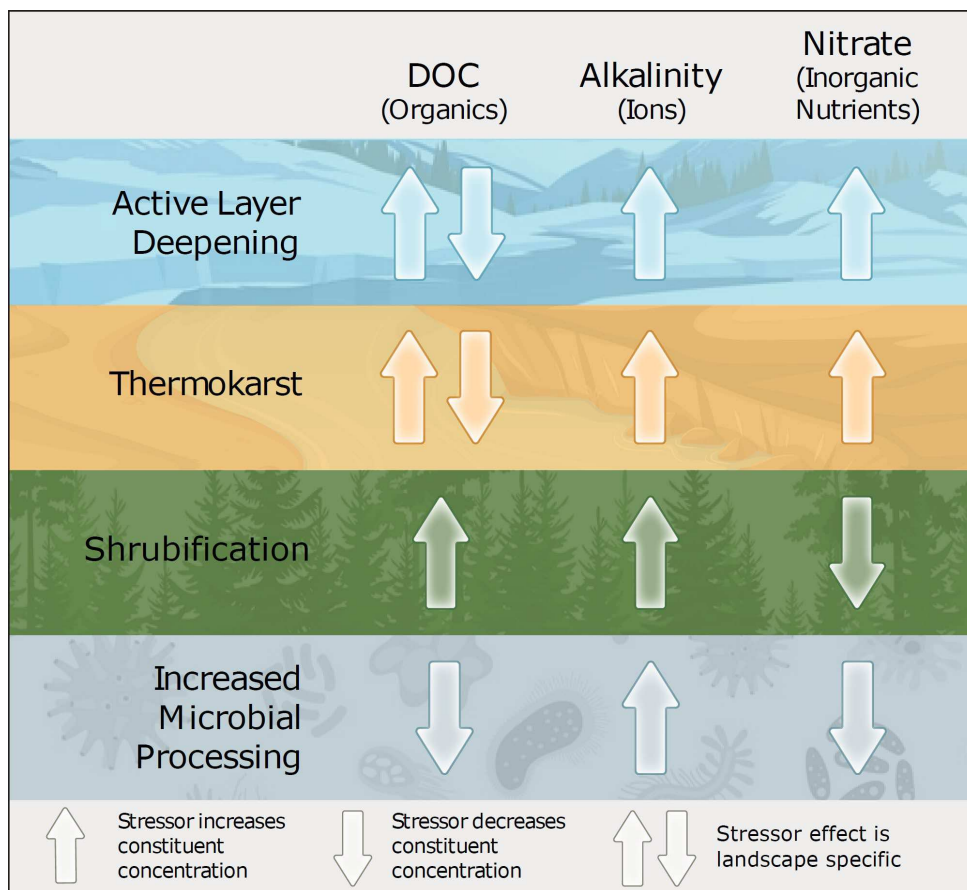


**Figure 5:** A conceptual diagram to illustrate key drivers of change of Arctic riverine chemistry, and their anticipated direction of effect for each of the three focal constituents. The Supplemental Text provides an overview of the literature evidence for this conceptual exercise, in addition to a description of drivers that are regional in their effect, or exert control largely outside of the timespan of the ArcticGRO data record.

176 For other constituents, variation in the directionality of factors of change appears to cause a  
 177 muted overall response. In the case of DOC, for example, permafrost thaw can either increase<sup>40</sup> or  
 178 decrease<sup>34</sup> loading to aquatic systems, depending on the composition of soils subject to thaw<sup>35</sup>. While  
 179 greening will increase vegetation and litter substrates for leaching and therefore the transport of  
 180 organic matter to aquatic networks<sup>41</sup>, temperature-driven increases in mineralization<sup>18,42</sup> and potential

181 rapid processing of novel organic matter substrates<sup>43</sup> act in opposition to this effect. Across these large  
182 Arctic rivers, the net result appears to be a dissipation of effect with transport through aquatic  
183 networks, and little net change in DOC delivery to the coastal ocean over the timespan of this  
184 assessment.

185 Finally, in some cases, geographically widespread processes appear to overwhelm counteracting  
186 drivers. For example, although we broadly expect permafrost thaw to increase inorganic nitrogen  
187 delivery to aquatic networks<sup>29</sup>, our analyses reveal declines in the transport of  $\text{NO}_3^-$  (and other inorganic  
188 nutrients) to the Arctic Ocean from large Arctic rivers. This suggests that factors such as temperature-  
189 driven increases in nitrogen cycling<sup>17</sup> or nitrogen uptake and/or immobilization<sup>16,44</sup> may currently be  
190 overwhelming local increases in mobilization<sup>29</sup>, when assessed at the large-river watershed scale. These  
191 findings underline the importance of taking a systems approach to understanding Arctic change, with an  
192 acknowledgement that biogeochemical cycles are inherently linked across elements and space.

193

#### 194 **Broad perturbation in linked biogeochemical cycles across the land-ocean Arctic domain**

195 Our analyses diagnose changes to the land-ocean Arctic system that are pervasive enough to leave few  
196 biogeochemically-active elements unscathed. As a result, these findings likely signal domain-scale  
197 change to ecosystem function. On land, ecosystem models have predicted increases in organic matter  
198 loading to fluvial networks in the changing north<sup>45</sup>. The lack of this signal at river outflows, therefore,  
199 suggests possible increases in carbon mineralization and associated outgassing during transit through  
200 watersheds, and thus an acceleration in carbon cycling within Arctic fluvial networks. Increasing  
201 alkalinity is suggestive of increases in chemical weathering, but in a region where a predominance of  
202 carbonate over silicate weathering, coupled with substantial sulfide oxidation in some watersheds,  
203 causes the ratio of  $\text{CO}_2$  consumption: alkalinity generation to be overall low relative to the global mean<sup>2</sup>.  
204 Increasing  $\text{SO}_4$  fluxes in rivers where  $\text{SO}_4$  appears to be largely derived from sulfides (Extended Data

205 Figure 3; Yukon, Kolyma<sup>46</sup>) may in fact indicate increasing bicarbonate liberation in the absence of CO<sub>2</sub>  
206 fixation<sup>2</sup>.

207 In the coastal ocean, riverine inputs of DIC result in CO<sub>2</sub> outgassing to the atmosphere<sup>47</sup>. The  
208 magnitude of this effect relative to weathering-induced CO<sub>2</sub> fixation on land, and its change, will play a  
209 key role in determining the carbon balance of the Arctic system. Acting concurrently, the declining NO<sub>3</sub><sup>-</sup>  
210 that we document is consistent with negative feedbacks for Arctic Ocean biological productivity and CO<sub>2</sub>  
211 uptake from the atmosphere, which is generally thought to be increasing as seasonal sea ice declines  
212 and nutrients become more available<sup>48</sup>. However, the Arctic Ocean also has globally low N:P ratios  
213 because its shelf sediments are a significant nitrogen sink through denitrification<sup>49</sup>. As a result,  
214 decreases in riverine NO<sub>3</sub><sup>-</sup> transport coupled with increasing discharge will increase stratification and  
215 decrease availability of nutrients for biological production. The changes will play out alongside other co-  
216 occurring processes, such as changes to the dilution effect of river water on ocean pH<sup>2</sup> with increasing  
217 alkalinity, and consequent effects of this change on primary production<sup>50</sup>.

218

## 219 **Conclusions**

220 In addition to implications for the current and future functioning of the land-ocean Arctic  
221 system, our findings point to several important considerations for understanding change. Particularly for  
222 bio-reactive constituents (DOC, nutrients), this work illustrates the importance of scale. Widespread  
223 declines in constituents such as NO<sub>3</sub><sup>-</sup> in the face of local processes known to increase land-water  
224 mobilization suggests a fulcrum-like redistribution in biogeochemical cycling at the landscape-scale,  
225 where fine-scale uptake and processing is increasing at the expense of communities downstream. How  
226 the balance between local mobilization and broader-scale processing may shift for the smaller  
227 catchments encircling the Arctic Ocean that have much shorter in-river transit times (see, for example,  
228 NO<sub>3</sub><sup>-</sup> trends in refs. <sup>51,52</sup>), or for other bio-reactive constituents (dissolved organic matter and other

229 inorganic nutrients) remains an open question. However, this potential scale-dependent variation in  
230 river mouth trends will be an important determinant of the geographic distribution of change in the  
231 Arctic nearshore. Teasing apart the relative importance of various drivers of change, and how they will  
232 vary with time and across constituents, will require process-based models, as already developed for  
233 alkalinity<sup>39</sup> and DOC<sup>45</sup>, in addition to models that are linked across elements and space<sup>47</sup>. These models  
234 must inherently co-consider multiple drivers of change, including those not directly discussed above  
235 (e.g., impoundment, declining acid deposition, land use and land cover change; see also Supplemental  
236 Text). The datasets we draw on for our analyses are remarkable for their geographic cohesion and their  
237 relative length. However, they also diagnose profound change occurring in real time. This work clearly  
238 calls for continued, coordinated observation of the land-ocean Arctic system. More importantly,  
239 however, it reinforces the need for rapid attention to Earth's warming climate, and its multiplicative  
240 effects in the north.

241

## 242 **Online Methods**

243

### 244 **Sample collection and dataset coverage**

245

246 *Water chemistry:* We began sampling the six largest Arctic rivers for water chemistry in the summer of  
247 2003. The project was initially called PARTNERS (Pan-Arctic River Transport of Nutrients, Organic Matter,  
248 and Suspended Sediments), and was expanded and renamed the Arctic Great Rivers Observatory  
249 (ArcticGRO) in 2008. Sample collection for the data presented in this paper occurred 5-7 times per year,  
250 with the exception of a short break during 2007-08 (Extended Data Figure 1). Water chemistry samples  
251 are collected as far downstream on each of the six Great Arctic rivers as logistically feasible, at Salekhard  
252 (Ob'), Dudinka (Yenisey), Zhigansk (Lena), Cherskiy (Kolyma), Pilot Station (Yukon), and Tsiigehtchic  
253 (Mackenzie) (Figure 1; Extended Data Table 1). Between 2003 and 2011, open water sampling was  
254 conducted using a D-96 sampler<sup>53</sup> equipped with a Teflon nozzle and Teflon sample collection bag,  
255 which enabled depth-integrated and flow-weighted samples. Samples were collected at five roughly  
256 equal increments across the river channel and combined in a 14-L Teflon churn, resulting in a single  
257 composite sample. Beginning in 2012, open-water sampling was conducted by collecting three near-  
258 surface samples on each of the left-bank, right-bank, and mid-points of each river, and combining these  
259 to form a composite sample. Across the full period of record, wintertime (under ice) samples were  
260 collected by drilling a hole at the river's mid-point, and collecting a sample from below the ice surface.

261

262 Within years, the timing of sample collection has changed slightly over the ArcticGRO period of record.  
263 Early collection schemes (2003-06 and 2009-11) focused on the spring freshet (three or more samples

264 per year), with further sample coverage through the more broadly-spread late summer (period of  
265 deepest thaw of the seasonally-frozen active layer; one to four samples) and winter (typically one  
266 sample) periods. Given the paucity of cross-site comparable data for these rivers at the outset of the  
267 ArcticGRO program, this sampling scheme was designed to maximize coverage during the high flows of  
268 the spring, when constituent concentrations are changing rapidly and the majority of constituent flux  
269 occurs<sup>54</sup>. In 2012, sampling shifted to become evenly spread across the annual cycle, with samples  
270 collected bi-monthly (i.e., six samples per year), and months of collection alternating between years.  
271 Sample processing (i.e., filtering and preservation) occurs within 24 hours of sample collection. As  
272 described above for sample collection, processing protocols were identical across all sites. Processed  
273 and preserved samples were shipped to Woods Hole, MA, where they were distributed to specialized  
274 laboratories for individual analyses. A complete description of processing and analytical methodologies  
275 is available on the ArcticGRO website ([www.arcticgreativers.org](http://www.arcticgreativers.org)), and archived at the Arctic Data  
276 Center<sup>55</sup>. The focal constituents highlighted in this paper were analyzed as follows: For DOC, on a  
277 Shimadzu TOC analyzer, following acidification with HCl, sparging, and using the 3 of 5 injections that  
278 resulted in the lowest coefficient of variation; for alkalinity, following acid titration using a Hach digital  
279 titrator (2003-2009) and Mettler Toledo model T50M titrator (2010 onwards); for NO<sub>3</sub><sup>-</sup> (as NO<sub>3</sub><sup>-</sup> + NO<sub>2</sub><sup>-</sup>)  
280 colorimetrically using a Lachat Quickchem FIA+ 8000 (2003-2011) and Astoria (2012 onwards)  
281 autoanalyzer.

282  
283 *Discharge:* All Arctic-GRO discharge measurements are from long-term gauging stations operated by  
284 Roshydromet, the US Geological Survey, and the Water Survey of Canada. On the Ob', Yukon, and  
285 Mackenzie Rivers, gauging stations are identical to the ArcticGRO sample collection location. On the  
286 Yenisey, Lena, and Kolyma Rivers, proximate gauging stations were used, at Kyusyur, Igarka, and  
287 Kolymskoye, respectively. The effect of this modest offset, and methods for correction, have been  
288 described elsewhere<sup>54</sup>. Continually-updated concentration and discharge datasets are available on the  
289 ArcticGRO website. Concentration and discharge data used for this analysis (i.e., 2003 – 2019, inclusive)  
290 have been archived at the Arctic Data Center (<https://doi.org/10.18739/A2VH5CK43>).

291

## 292 **Determination of constituent flux using the WRTDS Kalman approach**

293

294 Determining constituent flux requires a modelling approach, because discharge data are typically  
295 available at daily (or even more refined) time steps, while concentration measurements are almost  
296 always collected much more patchily over time. We used the Weighted Regressions on Time, Discharge,  
297 and Season (WRTDS) approach to estimate constituent flux over the ArcticGRO period of record,  
298 actualized in the *EGRET* (Exploration and Graphics for RivEr Trends)<sup>56</sup> package in the R statistical  
299 platform<sup>57</sup>. This approach has been shown to provide more accurate estimates of constituent flux than  
300 other common statistical techniques used for flux estimation<sup>58</sup>, as a result of the use of weighted  
301 regression (see below), and the removal of the requirement for homoscedastic residuals for bias  
302 correction<sup>59</sup>. Similar to other flux estimation techniques, the predictive equation takes the form of:

303

$$304 \ln(c) = \beta_0 + \beta_1 t + \beta_2 \ln(Q) + \beta_3 \sin(2\pi t) + \beta_4 \cos(2\pi t) + \varepsilon \quad (1)$$

305

306 where  $c$  is concentration,  $Q$  is discharge,  $t$  is time in decimal years, and  $\varepsilon$  is the unexplained variation,  
307 with the sine and cosine functions enabling seasonality within the model<sup>30</sup>. However, unlike most other  
308 flux modelling approaches, the coefficients  $\beta_0 - \beta_4$  are not static, but are allowed to vary gradually in  $Q, t$   
309 space. This is accomplished via an approach that develops a separate model for each day of the  
310 observational record by re-evaluating the relationship between concentration and time, season, and  
311 discharge, with a weighting that prioritizes samples closest in  $Q, t$  space to the day of estimation<sup>59</sup>. For



312 this work, we use the WRTDS-Kalman modification, which further improves upon the above-described  
313 technique by using a first order autoregressive (AR1) model to capture residual autocorrelation<sup>60</sup>. An  
314 assessment of measured vs. modelled daily outputs via WRTDS-Kalman is provided in Extended Data  
315 Figure 6. Daily WRTDS-Kalman flux outputs have been archived at the Arctic Data Center  
316 (<https://doi.org/10.18739/A2VH5CK43>).

317

### 318 **Calculation of flow-normalized flux, and assessment of flow-normalized trends**

319

320 A complication of evaluating trends in flux is that a substantial amount of variation in concentration is  
321 caused by year-to-year variation in discharge, which adds considerable noise to the time series. To  
322 assess changes in flux with year-to-year variation in discharge removed, we use the WRTDS *flow*  
323 *normalization* technique, which filters out the influence of inter-annual variation in streamflow. This is  
324 accomplished by creating a probability density function (pdf) of  $Q$  for each day of the calendar year, and  
325 producing flow-normalized concentrations and fluxes that integrates over this pdf<sup>32</sup>. In this way,  
326 discharge is normalized across calendar years, but intra-annual variation (i.e., seasonal variation, at a  
327 daily time step) is retained. Given the statistical complexity of this smoothing approach, we estimate  
328 uncertainty in change over the flow normalized time series using a block bootstrap technique  
329 implemented in the R package *EGRETCi*, which creates a posterior mean estimate ( $\hat{\pi}$ ) of the probability  
330 of a trend, and assesses trend likelihood as: highly likely ( $\hat{\pi} < 0.05$  or  $> 0.95$ ) very likely ( $\hat{\pi}$  0.05-0.10 or  
331 0.90-0.95), likely ( $\hat{\pi}$  0.10-0.33 or 0.66-0.90), or about as likely as not ( $\hat{\pi}$  0.33-0.66)<sup>32</sup>. Our results are  
332 provided as mean and 90% confidence interval outputs from the block bootstrap approach described in  
333 ref. <sup>32</sup>.

334

### 335 **Assessment of trends in annual discharge and WRTDS-Kalman constituent flux**

336

337 Daily discharge and flux estimates were summed within years to generate an annual time series, and a  
338 Mann-Kendall test was used to analyze the significance of annual trends over time. Within this analysis,  
339 trend slopes were calculated using the Theil-Sen method. Trend analyses, and the calculation of slopes  
340 were conducted using the *trend* package<sup>61</sup> in R<sup>57</sup>. We report Kendall's p-value and Sen's slope in the  
341 main text, and report additional statistical outputs in Table S1.

342

### 343 **Assessment of trends in concentration**

344 To allow us to examine trends in concentration directly, but account for seasonal variation in  
345 concentration measurements that may skew trend detection, we used a Seasonal Kendall test<sup>62</sup>. This  
346 approach accounts for seasonality by calculating the Mann-Kendall statistic for each of  $p$  seasons  
347 directly, and then combines the test statistic for each season ( $S_p$ ) to create an overall seasonal Kendall  
348 statistic ( $S'$ ):

349

$$S' = \sum_{i=1}^p S_p$$

350

351 We used a modification of the original seasonal Kendall test which accounts for serial dependence by  
352 using an autoregressive moving average (ARMA) (1:1) approach<sup>63</sup>. We defined seasons as spring (May-  
353 June), summer (July-October) and winter (November-April), as has been previously established for the  
354 ArcticGRO dataset<sup>54,64</sup>. We further used a seasonal Kendall slope estimator to determine the magnitude  
355 of trends, following the Theil-Sen approach as modified for the seasonal Kendall test<sup>62</sup>.

356

### 357 **Data visualization**

358 Figures 2-4 and Extended Data figures 1 and 3-5 were actualized in R<sup>57</sup> using *ggplot2*<sup>65</sup>. The correlation  
359 cluster analysis shown in Extended Data figure 2 was carried out using the function “heatmap.2” in the  
360 *gplots* package<sup>66</sup> in R.

361

### 362 **Data availability**

363 Data used for our analyses and daily Kalman outputs are provided as a fixed package at the Arctic Data  
364 Center (<https://doi.org/10.18739/A2VH5CK43>). More recent updates of the ArcticGRO water quality  
365 and discharge datasets can be found at the project website ([www.arcticgreativers.org](http://www.arcticgreativers.org)) and through the  
366 Arctic Data Center<sup>55</sup>.

367

### 368 **Acknowledgements**

369 Funding for the PARTNERS program and Arctic Great Rivers Observatory has been provided via NSF  
370 grants 0229302, 0732985, 0732821, 0732522, 0732583, 1107774, 1603149, 1602680, 1602615,  
371 1914081, 1914215, 1913888, and 1913962. This work would not have been possible without  
372 contributions from many individuals at the six ArcticGRO sampling locations, and we very gratefully  
373 acknowledge contributions from Edwin Amos, Bart Blais, Charlie Couvillion, Anya Davydova, Nicole Dion,  
374 Vladimir Efremov, Les Kutny, Ryan McLeod, Robert Myers, Alexander Pavlov, Alexander Smirnov, Mikhail  
375 Suslov, Galina Zimova, and support from the Environment and Climate Change Canada (ECCC) and  
376 Indigenous and Northern Affairs Canada (INAC) offices in Inuvik, Canada. We also would like to  
377 acknowledge that sample collection occurred within the Gwich'in Settlement Region (Mackenzie River),  
378 and on the traditional territories of the Yup'ik people (Yukon River) in North America and the Evenk  
379 people (Lena River) in Russia. Julianne Waite assisted with the creation of Figure 5. Sean Sylva, Gretchen  
380 Swarr, and Maureen Auro assisted with analyses of major and trace anion/cation data.

381

### 382 **Author contributions**

383 *Conceived of the paper and performed data analysis:* SET, RMH, JWM, RGMS, AS, FM, AIS; *Led*  
384 *manuscript preparation:* SET; *Initial design of the ArcticGRO (PARTNERS) program:* BJP, RMH, JWM, PAR,  
385 RGS, RMWA, LWC, VVG, SZ, AVZ; *Sample and data acquisition:* AVZ, TYG, SZ, NZ, GE, PFS, EAM, RS, MT,  
386 LSK; *Performed laboratory analyses:* AS, LS, BP-E, PR, CG, PFS; *Read and commented on the manuscript:*  
387 All authors

388

389 **Corresponding author:** Suzanne E. Tank ([suzanne.tank@ualberta.ca](mailto:suzanne.tank@ualberta.ca))

390

391 **Competing interests:** The authors declare no competing interests.

392

393

394 **Extended Data Table 1:** Characteristics of the six largest Arctic watersheds.

	Watershed Area	Area at gauge	Distance to Arctic Ocean <sup>a</sup>	Mean discharge <sup>b</sup>	Runoff	Permafrost <sup>c</sup>	Continuous Permafrost <sup>c</sup>	Discontinuous Permafrost <sup>c</sup>	Tundra <sup>d</sup>	Forest <sup>d</sup>	Regulated <sup>e</sup>	Mean annual temperature (2003-2019) <sup>f</sup>	Mean annual precipitation (2003-2019) <sup>f</sup>	Population Density <sup>g</sup>
	10 <sup>6</sup> km <sup>2</sup>	10 <sup>6</sup> km <sup>2</sup>	km	km <sup>3</sup> y <sup>-1</sup>	mm y <sup>-1</sup>	(% area)	(% area)	(% area)	(% area)	(% area)	(% area)	°C	mm y <sup>-1</sup>	people km <sup>-2</sup>
Ob'	2.99	2.95	287	409	139	26	2	4	0.1	48.2	14.6	-0.7	604	9.07
Yenisey	2.54	2.44	433 (697)	595	244	88	33	11	0.5	67.9	50.5	-4.4	619	2.85
Lena	2.46	2.43	754 (211)	599	247	99	79	11	1.2	62.5	7.2	-8.9	548	0.45
Kolyma	0.65	0.53	120 (283)	108	205	100	100	0	3.2	16.7	18.9	-10.7	546	0.2
Yukon	0.83	0.83	200	211	254	99	23	66	0.1	68.4	0.0	-4.8	571	0.17
Mackenzie	1.78	1.68	260	295	176	82	16	29	0.0	74.2	4.3	-3.6	547	0.25
Sum	11.25	--	--	2,217	--	--	--	--	--	--	--	--	--	--
Pan-Arctic	16.8 <sup>h</sup>	--	--	~3710 <sup>i</sup>	~220	--	--	--	--	--	--	--	--	--

395

396

397

<sup>a</sup> Distance from the water chemistry station (discharge gauge) to the Arctic Ocean, including transit distance through river mouth Deltas. Where only one value is presented, water chemistry and discharge data collection are co-located. Data for Russian rivers are from the Hydrometeorological Service of the USSR<sup>67</sup>. Data for North American rivers are estimated from Google Earth.

398

<sup>b</sup> Mean annual discharge over the study period

399

<sup>c</sup> From Holmes et al. (2013)<sup>68</sup>. Permafrost extent and classification from the International Permafrost Association's Circum-Arctic Map of Permafrost and Ground Ice Conditions.

400

<sup>d</sup> Vegetation classes from the 20-class GLDAS/NOAH product<sup>69</sup>, based on a 30 arc second MODIS vegetation data that uses a modified IGBP classification scheme. Tundra is the sum of mixed and bare ground tundra. Forest is the sum of evergreen, deciduous, and mixed forest, and wooded tundra.

401

402

<sup>e</sup> Regulated area at the end of the study period, from Lehner et al. (2011)<sup>70</sup>. Includes impoundments that were completed on the Kolyma (2013) and Yenisey (2012) rivers during the ArcticGRO period of analysis.

403

404

<sup>f</sup> Mean annual temperature and precipitation from the MERRA2 reanalysis product<sup>71</sup>.

405

<sup>g</sup> Population density from the Center for International Earth Science Information Network (2018)<sup>72</sup> gridded population of the world.

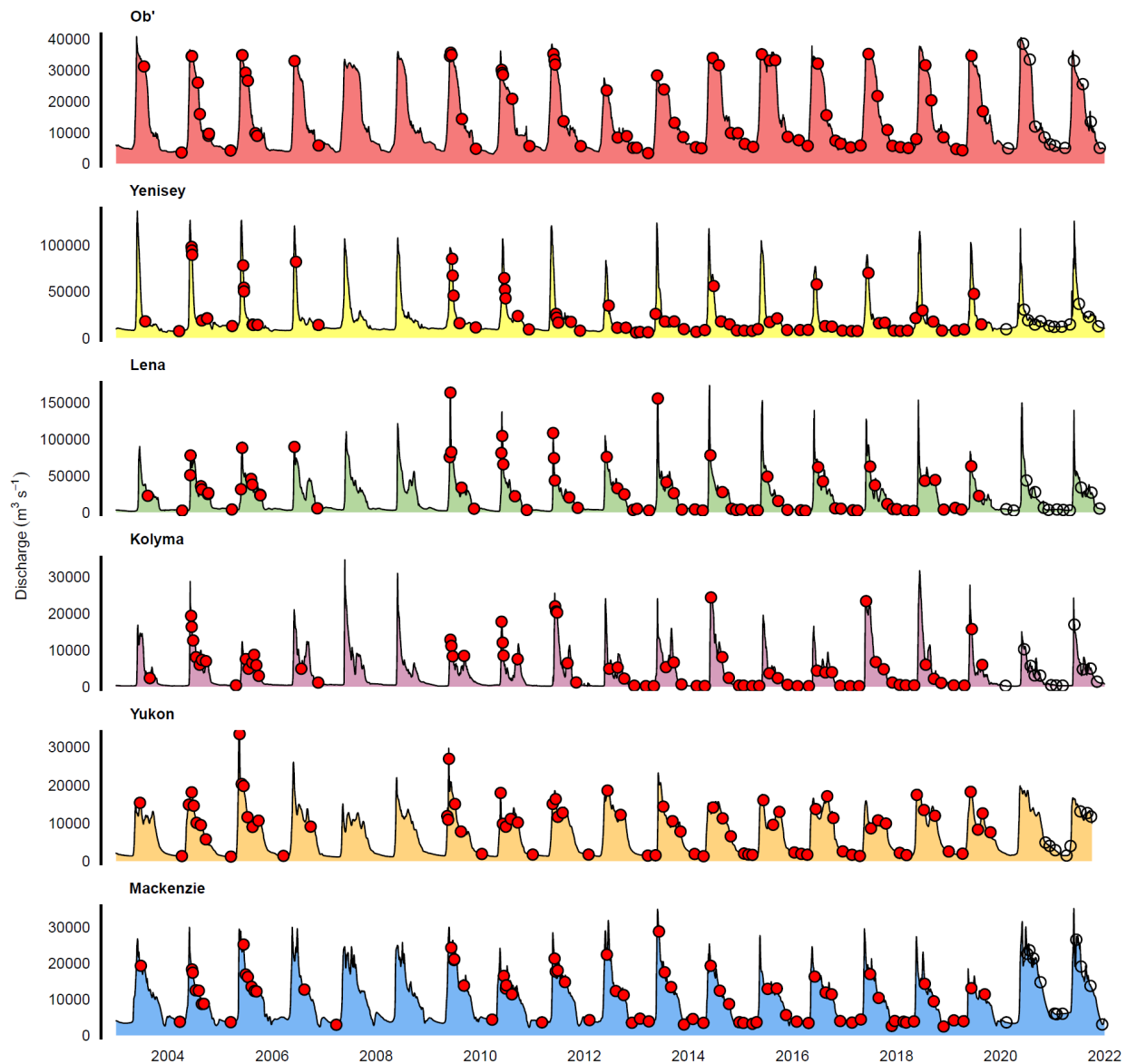
406

<sup>h</sup> Watershed area of 16.8 x 10<sup>6</sup> km<sup>2</sup> corresponds to the area demarcated in Figure 1, which does not include drainage to Hudson Bay. The pan-Arctic watershed including Hudson Bay, but excluding the Greenland Ice Cap, covers an area of 22.4 x 10<sup>6</sup> km<sup>2</sup> (from Lammers et al. 2001<sup>73</sup>)

407

408

<sup>i</sup> Estimate derived from Shiklomanov et al. 2021<sup>22</sup>, for the period covering 1980-2018



409

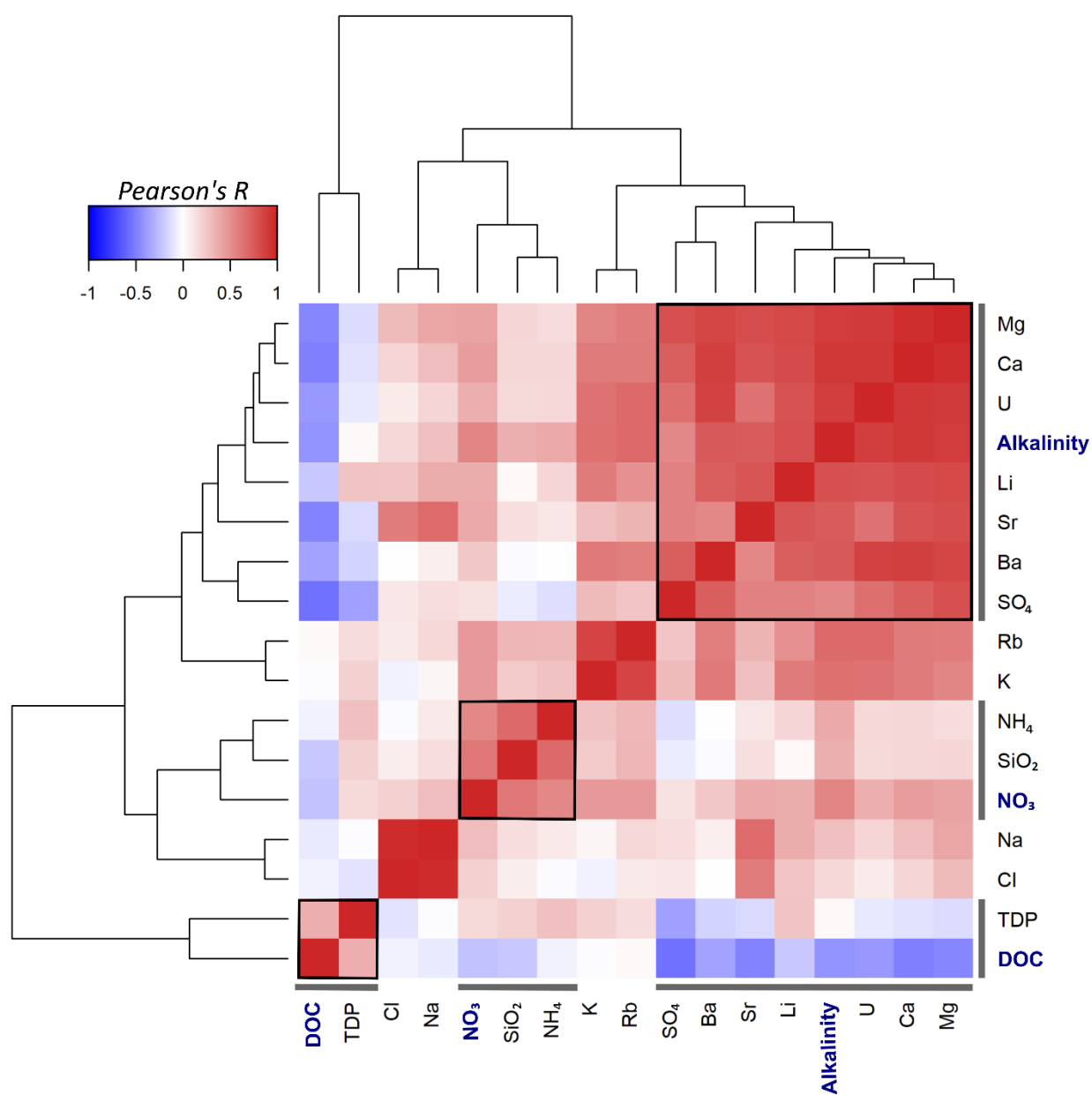
410

411 **Extended Data Figure 1:** Time-series of discharge and concentration measurements across the six Arctic  
 412 Great Rivers. Discharge is shown as a continuous time-series for all rivers. Dates of sample collection for  
 413 concentration measurements used in this analysis are shown with red circles; clear circles indicate  
 414 ongoing data collection.

415

416

417

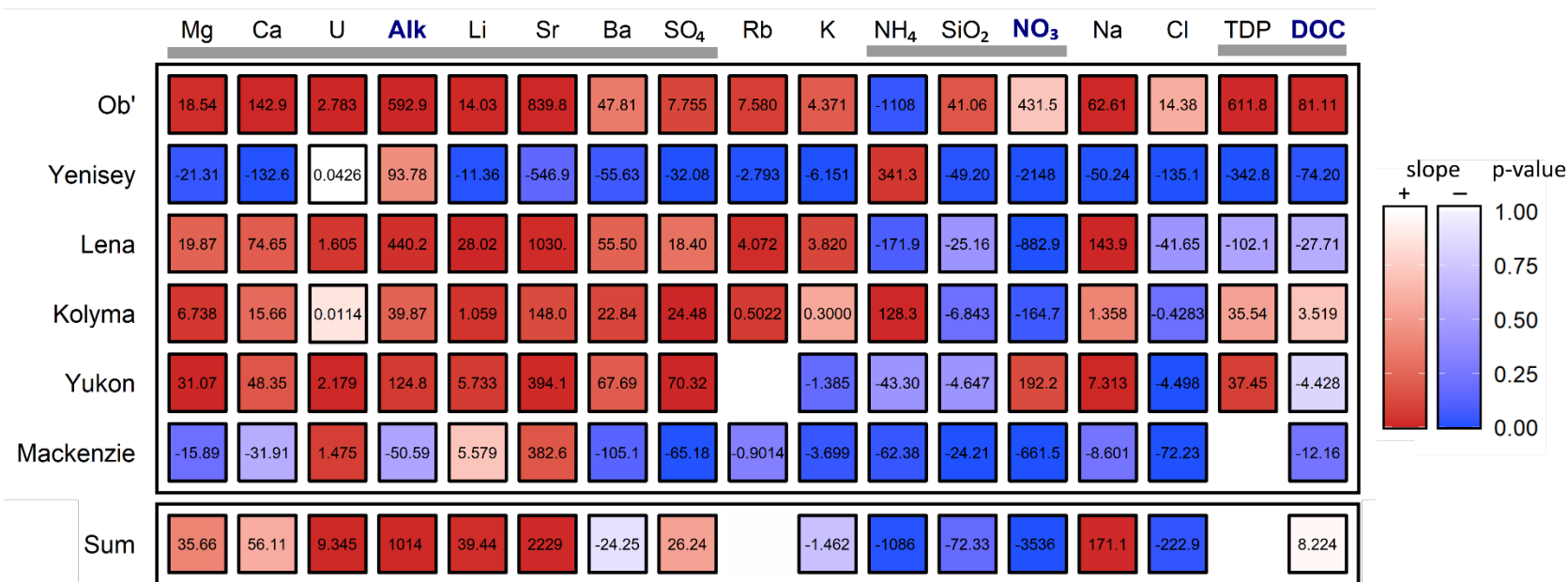


418

419 **Extended Data Figure 2:** A cluster heatmap illustrating correlation between constituents for the full  
420 ArcticGRO dataset. Shading indicates the Pearson correlation coefficient, which was used as the distance  
421 metric for hierarchical clustering. Focal constituents (alkalinity, nitrate [NO<sub>3</sub>-N], and dissolved organic  
422 carbon [DOC]) are bolded in blue. Black boxes within the correlation plot and grey shading along axes  
423 indicate clusters associated with each focal constituent.

424

425



426

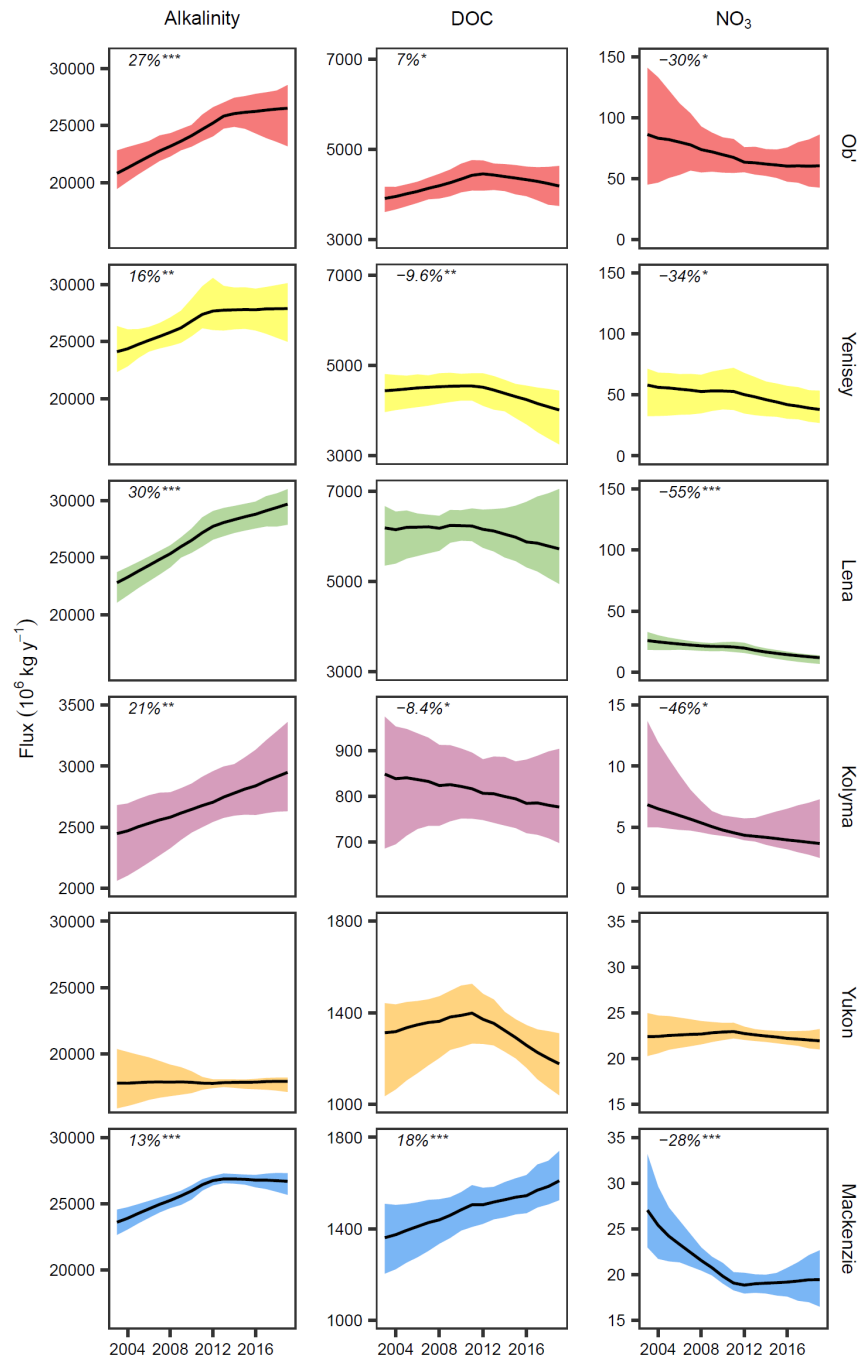
427

428

429

430

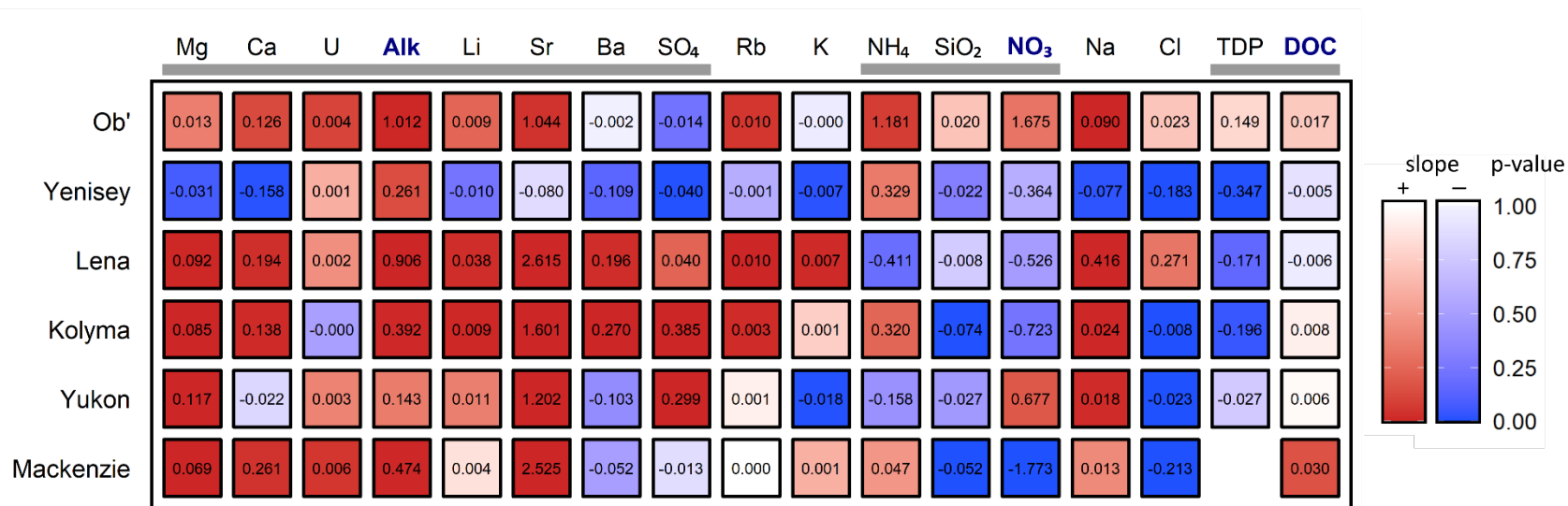
**Extended Data Figure 3:** Annual trends in constituent flux across the full ArcticGRO dataset, for each of the six great Arctic rivers. Trend analysis is via a Mann-Kendall analysis; the Thiel-Sen slope (numerical value) and p-value of the trend analysis (shading) are shown. Corresponding trends in concentration are provided in Extended Data Figure 5. Grey bars illustrate groupings from Extended Data Figure 2. Units ( $\text{Gg y}^{-1}$  or  $\text{Mg y}^{-1}$ ) are provided in Table S1.



432

433 **Extended Data Figure 4:** Flow-weighted trends in annual constituent flux for the three focal constituents  
 434 (alkalinity, dissolved organic carbon [DOC], and nitrate [ $\text{NO}_3\text{-N}$ ], for each of the six Great Arctic rivers.  
 435 The solid line indicates the mean, and shading indicates 90% confidence interval from the block  
 436 bootstrap analysis. Asterisks indicate trends that are: \*\*\*highly likely (posterior mean estimate  $\hat{\pi} < 0.05$  or  
 437  $> 0.95$ ); \*\*very likely ( $\hat{\pi}$  0.05-0.10 or 0.90-0.95); or \*likely ( $\hat{\pi}$  0.10-0.33 or 0.66-0.90), with percentage  
 438 change in constituent flux indicated for the period of record. Where no percentage change is shown,  
 439 trends were assessed to be about as likely as not ( $\hat{\pi}$  0.33-0.66).

440

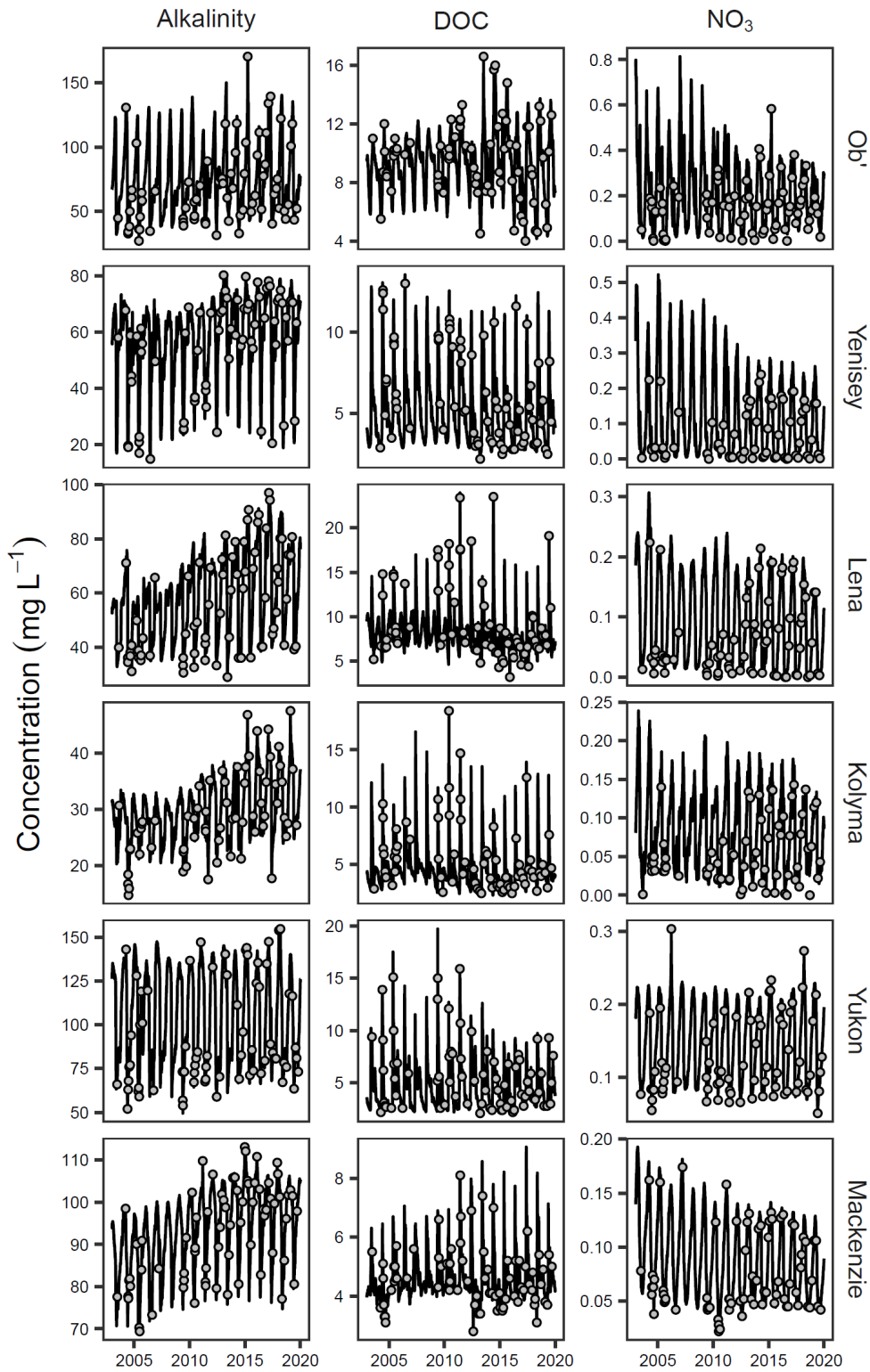


441

442

443 **Extended Data Figure 5:** Trends for constituent concentration across the full ArcticGRO dataset, for each of the six great Arctic rivers. Trend  
 444 analysis is via a seasonal Mann-Kendall analysis; the Thiel-Sen slope (numerical value) and p-value of the trend analysis (shading) are shown.  
 445 Corresponding trends in constituent flux are provided in Extended Data Figure 3. Grey bars illustrate groupings from Extended Data Figure 2.  
 446 Units (mg L<sup>-1</sup> y<sup>-1</sup> or µg L<sup>-1</sup> y<sup>-1</sup>) are provided in Table S2.





447

448 **Extended Data Figure 6:** Measured vs. modelled concentrations of the focal constituent suite, for each  
 449 of the six great Arctic rivers. Circles indicate true concentration measurements; lines indicate outputs  
 450 from the WRTDS-Kalman model.

451 **References**

- 452
- 453 1 Carmack, E. C. *et al.* Freshwater and its role in the Arctic Marine System: Sources, disposition,  
 454 storage, export, and physical and biogeochemical consequences in the Arctic and global oceans.  
 455 *J. Geophys. Res.-Biogeosci.* **121**, 675-717, doi:<https://doi.org/10.1002/2015JG003140> (2016).
- 456 2 Tank, S. E. *et al.* A land-to-ocean perspective on the magnitude, source and implication of DIC  
 457 flux from major Arctic rivers to the Arctic Ocean. *Global Biogeochem. Cycles* **26**, GB4018,  
 458 doi:[10.1029/2011GB004192](https://doi.org/10.1029/2011GB004192) (2012).
- 459 3 Dunton, K. H., Weingartner, T. & Carmack, E. C. The nearshore western Beaufort Sea ecosystem:  
 460 Circulation and importance of terrestrial carbon in arctic coastal food webs. *Progress in*  
 461 *Oceanography* **71**, 362–378 (2006).
- 462 4 Terhaar, J., Lauerwald, R., Regnier, P., Gruber, N. & Bopp, L. Around one third of current Arctic  
 463 Ocean primary production sustained by rivers and coastal erosion. *Nat. Commun.* **12**, 169,  
 464 doi:[10.1038/s41467-020-20470-z](https://doi.org/10.1038/s41467-020-20470-z) (2021).
- 465 5 McClelland, J. W., Holmes, R. M., Dunton, K. H. & Macdonald, R. W. The Arctic Ocean estuary.  
 466 *Estuar. Coast.* **35**, 353–368, doi:[10.1007/s12237-010-9357-3](https://doi.org/10.1007/s12237-010-9357-3) (2012).
- 467 6 Previdi, M., Smith, K. L. & Polvani, L. M. Arctic amplification of climate change: a review of  
 468 underlying mechanisms. *Environ. Res. Lett.* **16**, 093003, doi:[10.1088/1748-9326/ac1c29](https://doi.org/10.1088/1748-9326/ac1c29) (2021).
- 469 7 Peterson, B. J. *et al.* Increasing river discharge to the Arctic Ocean. *Science* **298**, 2171-2173  
 470 (2002).
- 471 8 McClelland, J. W., Dery, S. J., Peterson, B. J., Holmes, R. M. & Wood, E. F. A pan-arctic evaluation  
 472 of changes in river discharge during the latter half of the 20th century. *Geophys. Res. Lett.* **33**,  
 473 L06715, doi:[10.1029/2006GL025753](https://doi.org/10.1029/2006GL025753) (2006).
- 474 9 Rawlins, M. A. *et al.* Analysis of the Arctic system for freshwater cycle intensification:  
 475 Observations and expectations. *J. Clim.* **23**, 5715-5737, doi:[doi:10.1175/2010JCLI3421.1](https://doi.org/10.1175/2010JCLI3421.1) (2010).
- 476 10 Raymond, P. A. *et al.* Flux and age of dissolved organic carbon exported to the Arctic Ocean: A  
 477 carbon isotopic study of the five largest Arctic rivers. *Glob. Biogeochem. Cycles* **21**, GB4011,  
 478 doi:[10.1029/2007GB002934](https://doi.org/10.1029/2007GB002934) (2007).
- 479 11 Gómez-Gener, L., Hotchkiss, E. R., Laudon, H. & Sponseller, R. A. Integrating Discharge-  
 480 concentration dynamics across carbon forms in a boreal landscape. *Water Resour. Res.* **57**,  
 481 e2020WR028806, doi:<https://doi.org/10.1029/2020WR028806> (2021).
- 482 12 Toohey, R. C., Herman-Mercer, N. M., Schuster, P. F., Mutter, E. A. & Koch, J. C. Multidecadal  
 483 increases in the Yukon River Basin of chemical fluxes as indicators of changing flowpaths,  
 484 groundwater, and permafrost. *Geophys. Res. Lett.* **43**, 12,120-112,130,  
 485 doi:[10.1002/2016gl070817](https://doi.org/10.1002/2016gl070817) (2016).
- 486 13 Shogren, A. J. *et al.* Revealing biogeochemical signatures of Arctic landscapes with river  
 487 chemistry. *Sci Rep* **9**, 12894, doi:[10.1038/s41598-019-49296-6](https://doi.org/10.1038/s41598-019-49296-6) (2019).
- 488 14 Gabysheva, O. I., Gabyshev, V. A. & Barinova, S. Influence of the active layer thickness of  
 489 permafrost in eastern Siberia on the river discharge of nutrients into the Arctic Ocean. *Water* **14**,  
 490 84 (2022).
- 491 15 Tape, K., Sturm, M. & Racine, C. The evidence for shrub expansion in Northern Alaska and the  
 492 Pan-Arctic. *Global Change Biol.* **12**, 686-702, doi:[10.1111/j.1365-2486.2006.01128.x](https://doi.org/10.1111/j.1365-2486.2006.01128.x) (2006).
- 493 16 Reay, D. S., Nedwell, D. B., Priddle, J. & Ellis-Evans, J. C. Temperature dependence of inorganic  
 494 nitrogen uptake: reduced affinity for nitrate at suboptimal temperatures in both algae and  
 495 bacteria. *Appl. Environ. Microb.* **65**, 2577-2584, doi:[10.1128/AEM.65.6.2577-2584.1999](https://doi.org/10.1128/AEM.65.6.2577-2584.1999) (1999).
- 496 17 Salazar, A., Rousk, K., Jónsdóttir, I. S., Bellenger, J.-P. & Andrésón, Ó. S. Faster nitrogen cycling  
 497 and more fungal and root biomass in cold ecosystems under experimental warming: a meta-  
 498 analysis. *Ecology* **101**, e02938, doi:<https://doi.org/10.1002/ecy.2938> (2020).

499 18 Wickland, K. P. *et al.* Biodegradability of dissolved organic carbon in the Yukon River and its  
500 tributaries: Seasonality and importance of inorganic nitrogen. *Glob. Biogeochem. Cycles* **26**,  
501 GB0E03, doi:10.1029/2012gb004342 (2012).

502 19 Box, J. E. *et al.* Key indicators of Arctic climate change: 1971–2017. *Environ. Res. Lett.* **14**,  
503 045010, doi:10.1088/1748-9326/aafc1b (2019).

504 20 Maavara, T. *et al.* River dam impacts on biogeochemical cycling. *Nature Reviews Earth &*  
505 *Environment* **1**, 103-116, doi:10.1038/s43017-019-0019-0 (2020).

506 21 Zolkos, S. *et al.* Multidecadal declines in particulate mercury and sediment export from Russian  
507 rivers in the pan-Arctic basin. *Proc. Natl. Acad. Sci. USA* **119**, e2119857119,  
508 doi:doi:10.1073/pnas.2119857119 (2022).

509 22 Shiklomanov, A. *et al.* in *Arctic Hydrology, Permafrost and Ecosystems* (eds Daqing Yang &  
510 Douglas L. Kane) 703-738 (Springer International Publishing, 2021).

511 23 Bergen, K. M. *et al.* Long-term trends in anthropogenic land use in Siberia and the Russian Far  
512 East: a case study synthesis from Landsat. *Environ. Res. Lett.* **15**, 105007, doi:10.1088/1748-  
513 9326/ab98b7 (2020).

514 24 Aas, W. *et al.* Global and regional trends of atmospheric sulfur. *Sci Rep* **9**, 953,  
515 doi:10.1038/s41598-018-37304-0 (2019).

516 25 Slaveykova, V. I. Biogeochemical dynamics research in the Anthropocene. *Frontiers in*  
517 *Environmental Science* **7**, doi:10.3389/fenvs.2019.00090 (2019).

518 26 Vonk, J. E., Tank, S. E. & Walvoord, M. A. Integrating hydrology and biogeochemistry across  
519 frozen landscapes. *Nat. Commun.* **10**, 5377 (2019).

520 27 Opfergelt, S. The next generation of climate model should account for the evolution of mineral-  
521 organic interactions with permafrost thaw. *Environ. Res. Lett.* **15**, 091003, doi:10.1088/1748-  
522 9326/ab9a6d (2020).

523 28 Shakil, S., Tank, S. E., Vonk, J. E. & Zolkos, S. Low biodegradability of particulate organic carbon  
524 mobilized from thaw slumps on the Peel Plateau, NT, and possible chemosynthesis and sorption  
525 effects. *Biogeosciences* **19**, 1871-1890, doi:10.5194/bg-19-1871-2022 (2022).

526 29 Tank, S. E. *et al.* Landscape matters: Predicting the biogeochemical effects of permafrost thaw  
527 on aquatic networks with a state factor approach. *Permafrost Periglac.* **31**, 358-370,  
528 doi:https://doi.org/10.1002/ppp.2057 (2020).

529 30 Hirsch, R. M., Moyer, D. L. & Archfield, S. A. Weighted regressions on time, discharge, and  
530 season (WRTDS), with an application to Chesapeake Bay river inputs. *JAWRA Journal of the*  
531 *American Water Resources Association* **46**, 857-880, doi:https://doi.org/10.1111/j.1752-  
532 1688.2010.00482.x (2010).

533 31 Terhaar, J., Orr, J. C., Ethé, C., Regnier, P. & Bopp, L. Simulated Arctic Ocean response to  
534 doubling of riverine carbon and nutrient Delivery. *Glob. Biogeochem. Cycles* **33**, 1048-1070,  
535 doi:https://doi.org/10.1029/2019GB006200 (2019).

536 32 Hirsch, R. M., Archfield, S. A. & De Cicco, L. A. A bootstrap method for estimating uncertainty of  
537 water quality trends. *Environmental Modelling & Software* **73**, 148-166,  
538 doi:https://doi.org/10.1016/j.envsoft.2015.07.017 (2015).

539 33 Kokelj, S. V. & Jorgenson, M. T. Advances in thermokarst research. *Permafrost Periglac.* **24**, 108-  
540 119, doi:10.1002/ppp.1779 (2013).

541 34 Littlefair, C. A., Tank, S. E. & Kokelj, S. V. Retrogressive thaw slumps temper dissolved organic  
542 carbon delivery to streams of the Peel Plateau, NWT, Canada. *Biogeosciences* **14**, 5487-5505,  
543 doi:10.5194/bg-14-5487-2017 (2017).

544 35 Frey, K. E. & McClelland, J. W. Impacts of permafrost degradation on Arctic river  
545 biogeochemistry. *Hydrol. Process.* **23**, 169-182, doi:10.1002/hyp.7196 (2009).

546 36 Keller, K., Blum, J. D. & Kling, G. W. Stream geochemistry as an indicator of increasing  
547 permafrost thaw depth in an arctic watershed. *Chem. Geol.* **273**, 76-81 (2010).

548 37 Zolkos, S., Tank, S. E. & Kokelj, S. V. Mineral weathering and the permafrost carbon-climate  
549 feedback. *Geophys. Res. Lett.* **45**, 9623-9632, doi:doi:10.1029/2018GL078748 (2018).

550 38 Berner, R. A. The carbon cycle and CO<sub>2</sub> over Phanerozoic time: the role of land plants. *Philos.*  
551 *Trans. R. Soc. B-Biol. Sci.* **353**, 75-81, doi:10.1098/rstb.1998.0192 (1998).

552 39 Beaulieu, E., Godderis, Y., Donnadieu, Y., Labat, D. & Roelandt, C. High sensitivity of the  
553 continental-weathering carbon dioxide sink to future climate change. *Nature Clim. Change* **2**,  
554 346-349, doi:10.1038/nclimate1419 (2012).

555 40 Vonk, J. E. *et al.* High biolability of ancient permafrost carbon upon thaw. *Geophys. Res. Lett.* **40**,  
556 2689-2693, doi:10.1002/grl.50348 (2013).

557 41 Finstad, A. G. *et al.* From greening to browning: Catchment vegetation development and  
558 reduced S-deposition promote organic carbon load on decadal time scales in Nordic lakes. *Sci*  
559 *Rep* **6**, 31944, doi:10.1038/srep31944 (2016).

560 42 Moore, T. R., Paré, D. & Boutin, R. Production of dissolved organic carbon in Canadian forest  
561 soils. *Ecosystems* **11**, 740-751, doi:10.1007/s10021-008-9156-x (2008).

562 43 Drake, T. W. *et al.* The Ephemeral signature of permafrost carbon in an Arctic fluvial network. *J.*  
563 *Geophys. Res.-Biogeosci.* **123**, 1475-1485, doi:10.1029/2017jg004311 (2018).

564 44 Hicks Pries, C. E., McLaren, J. R., Smith Vaughn, L., Treat, C. & Voigt, C. in *Multi-scale*  
565 *Biogeochemical Processes in Soil Ecosystems: Critical Reactions and Resilience to Climate Change*  
566 (eds Y. Yu Yang, M. Keiluweit, N. Senesi, & B. Xing) (John Wiley & Sons, Inc., 2022).

567 45 Kicklighter, D. W. *et al.* Insights and issues with simulating terrestrial DOC loading of Arctic river  
568 networks. *Ecol. Appl.* **23**, 1817-1836, doi:https://doi.org/10.1890/11-1050.1 (2013).

569 46 Burke, A. *et al.* Sulfur isotopes in rivers: Insights into global weathering budgets, pyrite  
570 oxidation, and the modern sulfur cycle. *Earth Planet. Sc. Lett.* **496**, 168-177,  
571 doi:https://doi.org/10.1016/j.epsl.2018.05.022 (2018).

572 47 Lacroix, F., Ilyina, T. & Hartmann, J. Oceanic CO<sub>2</sub> outgassing and biological production hotspots  
573 induced by pre-industrial river loads of nutrients and carbon in a global modeling approach.  
574 *Biogeosciences* **17**, 55-88, doi:10.5194/bg-17-55-2020 (2020).

575 48 Lewis, K. M., van Dijken, G. L. & Arrigo, K. R. Changes in phytoplankton concentration now drive  
576 increased Arctic Ocean primary production. *Science* **369**, 198-202,  
577 doi:doi:10.1126/science.aay8380 (2020).

578 49 Chang, B. X. & Devol, A. H. Seasonal and spatial patterns of sedimentary denitrification rates in  
579 the Chukchi sea. *Deep Sea Research Part II: Topical Studies in Oceanography* **56**, 1339-1350,  
580 doi:https://doi.org/10.1016/j.dsr2.2008.10.024 (2009).

581 50 Dutkiewicz, S. *et al.* Impact of ocean acidification on the structure of future phytoplankton  
582 communities. *Nature Climate Change* **5**, 1002-1006, doi:10.1038/nclimate2722 (2015).

583 51 McClelland, J. W., Stieglitz, M., Pan, F., Holmes, R. M. & Peterson, B. J. Recent changes in nitrate  
584 and dissolved organic carbon export from the upper Kuparuk River, North Slope, Alaska. *J.*  
585 *Geophys. Res.-Biogeosci.* **112**, G04S60, doi:10.1029/2006JG000371 (2007).

586 52 Kendrick, M. R. *et al.* Linking permafrost thaw to shifting biogeochemistry and food web  
587 resources in an Arctic river. *Global Change Biol.* **24**, 5738-5750, doi:10.1111/gcb.14448 (2018).

588 53 Davis, B. E. A guide to the proper selection and use of federally approved sediment and water-  
589 quality samplers. Report No. 2005-1087, (2005).

590 54 Holmes, R. M. *et al.* Seasonal and annual fluxes of nutrients and organic matter from large rivers  
591 to the Arctic Ocean and surrounding seas. *Estuar. Coast.* **35**, 369-382, doi:10.1007/s12237-011-  
592 9386-6 (2012).

593 55 Holmes, R. M., McClelland, J., Tank, S., Spencer, R. & Shiklomanov, A. Arctic Great Rivers  
594 Observatory IV Biogeochemistry and Discharge Data: 2020-2024. Arctic Data Center.  
595 doi:10.18739/A2XW47X7D (2022).

596 56 Hirsch, R. M. & De Cicco, L. A. User guide to Exploration and Graphics for RivEr Trends (EGRET)  
597 and dataRetrieval: R packages for hydrologic data. Report No. 4-A10, 104 (Reston, VA, 2015).  
598 57 R Core Team. (R Foundation for Statistical Computing, Vienna, Austria, 2022).

599 58 Lee, C. J. *et al.* An evaluation of methods for estimating decadal stream loads. *J. Hydrol.* **542**,  
600 185-203, doi:https://doi.org/10.1016/j.jhydrol.2016.08.059 (2016).

601 59 Hirsch, R. M. Large biases in regression-based constituent flux estimates: Causes and diagnostic  
602 tools. *JAWRA Journal of the American Water Resources Association* **50**, 1401-1424,  
603 doi:https://doi.org/10.1111/jawr.12195 (2014).

604 60 Zhang, Q. & Hirsch, R. M. River Water-quality concentration and flux estimation can be  
605 improved by accounting for serial correlation through an autoregressive model. *Water Resour.*  
606 *Res.* **55**, 9705-9723, doi:https://doi.org/10.1029/2019WR025338 (2019).

607 61 trend: Non-Parametric Trend Tests and Change-Point Detection. R package version 1.1.4. (2020).

608 62 Hirsch, R. M., Slack, J. R. & Smith, R. A. Techniques of trend analysis for monthly water quality  
609 data. *Water Resour. Res.* **18**, 107-121, doi:https://doi.org/10.1029/WR018i001p00107 (1982).

610 63 Hirsch, R. M. & Slack, J. R. A Nonparametric trend test for seasonal data with serial dependence.  
611 *Water Resour. Res.* **20**, 727-732, doi:https://doi.org/10.1029/WR020i006p00727 (1984).

612 64 McClelland, J. W. *et al.* Particulate organic carbon and nitrogen export from major Arctic rivers.  
613 *Glob. Biogeochem. Cycles* **30**, 629-643, doi:10.1002/2015gb005351 (2016).

614 65 Wickham, H. *ggplot2: Elegant Graphics for Data Analysis*. (Springer-Verlag, 2016).

615 66 Warnes, G. R. *et al.* *gplots: Various R Programming Tools for Plotting Data*. R package version  
616 3.1.3. https://CRAN.R-project.org/package=gplots. (2022).

617 67 *The Resources of Surface Waters of the USSR. Hydrological Knowledge.*, Vol. 15, 16, 17, 19  
618 (Gidrometeoizdat, 1965-1969).

619 68 Holmes, R. M. *et al.* in *Climatic Change and Global Warming of Inland Waters: Impacts and*  
620 *Mitigation for Ecosystems and Societies* (eds C.R. Goldman, M. Kumagi, & R.D. Robarts) (Wiley,  
621 2013).

622 69 Rodell, M. *et al.* The global land data assimilation system. *Bulletin of the American*  
623 *Meteorological Society* **85**, 381-394 (2004).

624 70 Lehner, B. *et al.* High-resolution mapping of the world's reservoirs and dams for sustainable  
625 river-flow management. *Front. Ecol. Environ.* **9**, 494-502, doi:https://doi.org/10.1890/100125  
626 (2011).

627 71 Gelaro, R. *et al.* The modern-era retrospective analysis for research and applications, Version 2  
628 (MERRA-2). *J. Clim.* **30**, 5419-5454, doi:10.1175/jcli-d-16-0758.1 (2017).

629 72 Center for International Earth Science Information Network - CIESIN - Columbia University.  
630 (NASA Socioeconomic Data and Applications Center (SEDAC), Palisades, New York, 2018).

631 73 Lammers, R. B., Shiklomanov, A. I., Vorosmarty, C. J., Fekete, B. M. & Peterson, B. J. Assessment  
632 of contemporary Arctic river runoff based on observational discharge records. *J. Geophys. Res.-*  
633 *Atmos.* **106**, 3321-3334 (2001).

## Supplementary Files

This is a list of supplementary files associated with this preprint. Click to download.

- [AGROLongTermChangeSupplement20230130.pdf](#)